Analysis of the swimming of long and narrow animals

By Sir Geoffrey Taylor, F.R.S.

(*Received* 23 *February* 1952)

The swimming of long animals like snakes, eels and marine worms is idealized by considering the equilibrium of a flexible cylinder immersed in water when waves of bending of constant amplitude travel down it at constant speed. The force of each element of the cylinder is assumed to be the same as that which would act on a corresponding element of a long straight cylinder moving at the same speed and inclination to the direction of motion. Relevant aerodynamic data for smooth cylinders are first generalized to make them applicable over a wide range of speed and cylinder diameter. The formulae so obtained are applied to the idealized animal and a connexion established between B/λ, V/U and R_1. Here B and λ are the amplitude and wave-length, V the velocity attained when the wave is propagated with velocity U, R_1 is the Reynolds number $Ud\rho/\mu$, where d is the diameter of the cylinder, ρ and μ are the density and viscosity of water.

The results of calculation are compared with James Gray's photographs of a swimming snake and a leech.

The amplitude of the waves which produce the greatest forward speed for a given output of energy is calculated and found, in the case of the snake, to be very close to that revealed by photographs.

Similar calculations using force formulae applicable to rough cylinders yield results which differ from those for smooth ones in that when the roughness is sufficiently great and has a certain directional character propulsion can be achieved by a wave of bending which is propagated forward instead of backward. Gray's photographs of a marine worm show that this remarkable method of propulsion does in fact occur in the animal world.

1. Introduction

The motions which fishes, snakes and other animals make when they swim have been studied photographically by Gray (1939*a*). The way in which their muscles produce the observed movements of their flexible bodies seems to be understood. The external mechanics of the locomotion of snakes on land has also been discussed (Gray 1946, 1949), but attempts to analyze swimming from the point of view of hydrodynamics have failed because, in general, there is no way in which experiments made with rigid bodies can be used to predict the forces acting on flexible bodies. In the special case when the flexible body is very long compared with its lateral dimensions it may be legitimate to assume that the reaction of the surrounding water on any section or it is the same as though that section were part of a long cylinder moving at the same speed and in the same direction as itself. This assumption has been used successfully in calculating the curves made by the cable of a captive balloon in a wind or by the underwater part of a fishing line when trolling for mackerel. The data on which these calculations were based were obtained by setting up a long straight cylinder or wire at various angles of incidence to the air current in a wind-tunnel and measuring the force acting on it.

Attempts to apply similar methods to the mechanics of swimming might be successful if the swimmer were sufficiently long in comparison with its thickness. For this reason the swimming of snakes, leeches and certain marine worms have been studied. Since wind-tunnel measurements give the force on a cylinder set at angle of incidence i in a wind of velocity Q, the most direct method of applying the

Downloaded from https://royalsocietypublishing.org/ on 21 November 2023

Downloaded from https://royalsocietypublishing.org/ on 21 November 2023

basic assumptions would be to measure the velocity and direction of motion of each element of the body of a swimming animal at successive intervals of time. This could be done by making measurements on successive frames of a cinematograph record, but the work would be very laborious, and it might be impossible to make measurements sufficiently accurate to determine reliable values of Q and i. Even if the work could be carried out and the basic assumption used in conjunction with wind-tunnel measurements to calculate the force on each element of the body, the only possible final result would consist in verifying (or not verifying) that the integrated resultant force and couple acting on the whole animal are both zero. Such a result would contribute little to our understanding of the general principles of the mechanics of swimming.

For this reason a less direct method has been adopted. A study of successive frames in some of Gray's photographs of long animals swimming has revealed two main features which seem likely to be significant in the mechanics of swimming: (1) the animal sends waves of lateral displacement down its body and (2) in some cases, particularly in the case of a snake, these waves increase in amplitudes as they pass down the body.

In the analysis which forms the subject of this work the first of these features is studied as a problem in the mechanics of an idealized or 'mathematical' animal which consists of a flexible cylinder of uniform section. It will be assumed to swim by sending waves of uniform length and amplitude at a uniform speed down its body.

The work is divided into nine sections. In §2 the relevant aerodynamic data are examined and formulae are given for the lateral and longitudinal components of force acting on a cylinder set obliquely to a stream of fluid. Two sets of formulae are given. The first refers to smooth and the second to rough cylinders. In §3 equations are given which represent the geometry of a flexible cylinder down which waves of bending of constant amplitude are being propagated. In §4 the swimming characteristics of a smooth flexible cylinder are calculated and the results shown in a 'swimming diagram'. In §5 measurements of Gray's photographs of smooth animals swimming are compared with the calculations of §4. In §6 the energy required for propulsion of smooth animals is calculated and the amplitudes of the waves which drive them fastest for a given output of energy is found. In §7 calculations analogous to those of §4 are made for animals with a rough surface. It is found that when the surface is sufficiently rough and the roughness has certain directional characteristics, an animal could swim forwards by sending waves *forwards* along its body, and in §8 the performance of a marine worm which actually swims in this way is compared with the calculations. In §9 some limitations to the application of the analysis are mentioned and the swimming characteristics of a very small animal discussed.

2. The force on a circular cylinder set obliquely to a stream of fluid

Very few experimental data have been published on this subject. Relf & Powell (1917) gave measurements of the force on a smooth cylinder $\frac{3}{8}$ in. in diameter set at angles varying by 10° intervals from 0 to 90° to the wind direction. The transverse

force, F_N, and the longitudinal force, F_L, expressed as pounds weight per foot run of the cylinder in a wind of 40 ft./s, is given in table 1 (from Relf & Powell 1917).

TABLE 1. FORCE ON AN INCLINED CYLINDER $\frac{3}{8}$ INCH DIAMETER IN A WIND 40 FT./S

1	2	3	4	5	6	7
$i°$	F_N (Lb./ft. run)	F_L (Lb./ft. run)	$0{\cdot}07 \sin^2 i$	F_N (calc.)	$\frac{F_L}{\cos i(\sin i)^{\frac{1}{2}}}$	$\frac{F_L}{\cos i}$
0	0	0·0016	0	0	—	0·0016
10	0·0025	0·0016	0·0021	0·0021	0·0039	0·0016
20	0·0090	0·0021	0·0081	0·0081	0·0038	0·0022
30	0·0191	0·0024	0·0175	0·0172	0·0039	0·0029
40	0·0297	0·0023	0·0290	0·0282	0·0037	0·0030
50	0·0415	0·0019	0·0410	0·0400	0·0034	0·0029
60	0·0525	0·0015	0·0525	0·0509	0·0032	0·0030
70	0·0606	0·0012	0·0618	0·0598	0·0036	0·0035
80	0·0657	0·0003	0·0680	0·0657	[0·0017]	0·0017
90	0·0672	0	0·0700	0·0677	—	—

$$F_N \text{ (calc.)} = 5{\cdot}91 \times 10^{-2} \{1{\cdot}1 \sin^2 i + 0{\cdot}045 (\sin i)^{\frac{1}{2}}\}$$

It was pointed out by Relf & Powell that F_N is nearly proportional to $\sin^2 i$, where i is the angle between the axis of the cylinder and the wind direction. The values of $0{\cdot}07/\sin^2 i$ are given in column 4 of table 1 for comparison with values of F_N in column 2. It will be seen that the agreement is fairly good. If Q is the wind velocity $Q \sin i$ is the component of velocity at right angles to the cylinder, and since the drag on a cylinder placed at right angles to the wind is very nearly proportional to Q^2, the interpretation of their measurements, which Relf & Powell gave, is that the normal component of velocity determines the normal force independently of the longitudinal component $Q \cos i$. This result was to be expected on theoretical grounds because at the Reynolds number of Relf & Powell's experiments ($7{\cdot}9 \times 10^3$) the boundary layer is laminar. The field of flow is therefore one in which the three components of velocity u, v, w and also the pressure, p, are functions of two variables x and y only. Under these circumstances u, v and p are independent of w in the sense that their values are unaltered by any change in w, though w is dependent on u and v.

Relf & Powell's measurements were successfully used by McLeod (1918) to calculate the shape of a flexible cable used for towing weights under an aeroplane. For this purpose McLeod found that sufficiently accurate results could be obtained if F_L were neglected altogether. There is, however, an intrinsic interest in applying the principle that the transverse components of velocity are independent of the longitudinal components, to make predictions about the longitudinal force (Sears 1948; Wild 1949). In the present investigation the longitudinal component of force turns out to be of paramount importance. It is not possible to apply Relf & Powell's data directly to cases in which the Reynolds number differs greatly from that at which their experiments were made. For this reason, as well as for the intrinsic interest of the subject, a theoretical prediction about the effect of Reynolds number on the force acting on a cylinder placed obliquely in a stream of fluid is needed.

Downloaded from https://royalsocietypublishing.org/ on 21 November 2023

Normal component of force

The component of force acting on unit length of a cylinder at right angles to its axis when placed obliquely in a fluid stream will be represented by N, and N depends only on $Q \sin i$ so far as variations in Q and i are concerned.

The experimental results on smooth cylinders set at right angles to a fluid stream of velocity Q are represented in figure 1 (from Goldstein 1938). In this figure the drag coefficient C_D is plotted against $R = dQ\rho/\mu$; C_D is defined by the equation

$$N = \tfrac{1}{2}\rho Q^2 d C_D, \tag{2·1}$$

and $d = 2a$ is the diameter of the cylinder, ρ is the density of fluid and μ the viscosity. Curve a, figure 1, shows the value of C_D. Figure 1 also shows in b the part, $[C_D]_p$, of C_D which is due to the component of stress normal to the surface of the cylinder and in c the part $[C_D]_f$ due to the tangential component. Evidently

$$[C_D]_p + [C_D]_f = C_D. \tag{2·2}$$

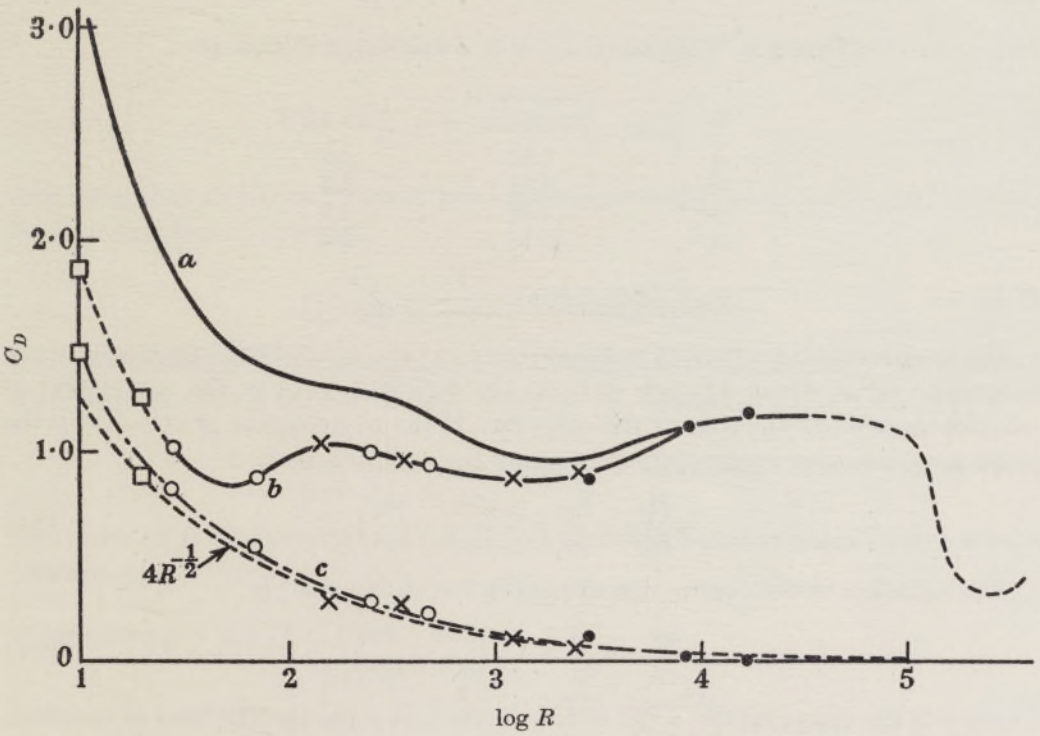

FIGURE 1. Drag coefficients for smooth circular cylinders.

It will be seen in figure 1 that $[C_D]_p$ is nearly constant in the range $20 < R < 10^5$, where it varies only between 0·9 and 1·1. On the other hand, $[C_D]_f$ is found to be nearly equal to $4R^{-\frac{1}{2}}$ in this range (Thom 1928). Using this value for $[C_D]_f$ the principle that lateral components of velocity are independent of longitudinal components yields the following expression for N:

$$N = \tfrac{1}{2}\rho d Q^2 \{[C_D]_p \sin^2 i + 4R^{-\frac{1}{2}} \sin^{\frac{3}{2}} i\}. \tag{2·3}$$

Downloaded from https://royalsocietypublishing.org/ on 21 November 2023

In Relf & Powell's experiments $R = 7{\cdot}9 \times 10^3$, so that $4R^{-\frac{1}{2}} = 0{\cdot}045$. Their measurements of F_N are expressed in Lb./ft. at 40 ft./s, so that the factor of C_D in (2·1) is

$$\frac{30{\cdot}48}{981 \times 453{\cdot}6}\left(\tfrac{1}{2}\right)(0{\cdot}00122)\left(\tfrac{3}{8} \times 2{\cdot}54\right)(40 \times 30{\cdot}48)^2 = 5{\cdot}91 \times 10^{-2}$$

and (2·3) gives

$$F_N = 5{\cdot}91 \times 10^{-2}\{[C_D]_p \sin^2 i \times 0{\cdot}045 \sin^{\frac{1}{2}} i\}. \tag{2·4}$$

The value of $[C_D]_p$ which, when $i = 90°$, gives the best agreement with the measurements of column 2, table 1, is $[C_D]_p = 1{\cdot}1$. Using this value in (2·4) the figures given in column 5, table 1, were calculated. Comparing columns 2 and 5 it will be seen that (2·3) is a good representation of Relf & Powell's measurements.

It is of interest to note that when $i = 90°$ (2·3) applies approximately to very low Reynolds numbers. The value of C_D for values of R from 0·4 to 4·0 has recently been calculated by Tomotika (1951). The corresponding values of $C_D = 1{\cdot}0 + 4R^{-\frac{1}{2}}$ which result from taking $[C_D]_p = 1$ in (2·3) are given in table 2 for comparison. It will be seen that when $i = 90°$ no large error will result from applying (2·3) down to $R = 2$.

TABLE 2. VALUES OF C_D FOR A CIRCULAR CYLINDER

R	Tomotika's calculation	$1{\cdot}0 + 4R^{-\frac{1}{2}}$
1	5·93	5·0
2	4·04	3·8
3	3·39	3·3
4	2·92	3·0

Longitudinal component of force L

The longitudinal component is due entirely to the longitudinal component of the tangential stress which depends only on the distribution of w, the component of velocity parallel to the axis of the cylinder. If the components of velocity in the plane perpendicular to this axis are u and v the equation for w is

$$u\frac{\partial w}{\partial x} + v\frac{\partial w}{\partial y} = \frac{\mu}{\rho}\left(\frac{\partial^2 w}{\partial x^2} + \frac{\partial^2 w}{\partial y^2}\right). \tag{2·5}$$

The equation to the conduction of heat in two dimensions is

$$u\frac{\partial \vartheta}{\partial x} + v\frac{\partial \vartheta}{\partial y} = \frac{\kappa}{\rho\sigma}\left(\frac{\partial^2 \vartheta}{\partial x^2} + \frac{\partial^2 \vartheta}{\partial y^2}\right), \tag{2·6}$$

where ϑ is the temperature, κ the conductivity and σ the specific heat at constant pressure. Since u and v are independent of w, (2·5) and (2·6) show that if $\kappa = \mu\sigma$ the equations for ϑ and w are identical. Though in fact for air $\kappa = 1{\cdot}14\mu\sigma$, it is worth while to make the assumption that $\kappa = \mu\sigma$ in order to make use of this analogue.

The boundary conditions to be satisfied at the surface of the cylinder are

$$\vartheta = \vartheta_0, \quad w = 0,$$

and at infinity

$$\vartheta = 0, \quad w = W.$$

Here ϑ is the excess of the temperature at any point above the air at distant points and ϑ_0 is the value of ϑ at the surface. W is the longitudinal component of velocity

Downloaded from https://royalsocietypublishing.org/ on 21 November 2023

of the air far from the cylinder which is taken to be at rest. The analogue therefore shows that at all points of the field

$$\frac{W-w}{W} = \frac{\vartheta}{\vartheta_0}. \tag{2·7}$$

The rate of loss of heat from unit length of the cylinder is $H = \kappa \int \frac{\partial \vartheta}{\partial n} \mathrm{d}s$, and the longitudinal force is $L = \mu \int \frac{\partial w}{\partial n} \mathrm{d}s$, the integrations being taken round the perimeter of a cross-section. Hence

$$\frac{L}{H} = \frac{\mu}{\kappa} \frac{W}{\vartheta_0}. \tag{2·8}$$

It is therefore possible to use measurements of H to determine L.

As a result of a large number of measurements of the rate of loss of heat from wires stretched at right angles to a wind stream, King (1914) concluded that the rate of loss of energy per unit length of wire of radius a is $1{\cdot}432 \times 10^{-3} \vartheta_0 \sqrt{(aQ)}$ watts. Dividing by 4·18 King's experimental result is therefore

$$\frac{H}{\vartheta_0} = 3{\cdot}417 \times 10^{-4} \sqrt{(aQ)} \text{ cal/s}. \tag{2·9}$$

Hence if $\kappa = \mu\sigma$,

$$\frac{L}{W} = 3{\cdot}14 \times 10^{-4} \frac{\mu}{\kappa} \sqrt{(aQ)}. \tag{2·10}$$

Assuming that air has no viscosity but has conductivity, Boussinesq (1905) obtained for heat loss from a cylinder

$$\frac{H}{\vartheta_0 \sqrt{(aQ)}} = \frac{8}{\sqrt{\pi}} \sqrt{(\rho\kappa\sigma)} = 4{\cdot}51 \sqrt{(\rho\kappa\sigma)}. \tag{2·11}$$

King, on the other hand, made the same assumption about viscosity but assumed a different surface condition of heat transfer. His theoretical result was

$$\frac{H}{\vartheta_0 \sqrt{(aQ)}} = 2\sqrt{\pi} \sqrt{(\rho\kappa\sigma)} = 3{\cdot}55 \sqrt{(\rho\kappa\sigma)}. \tag{2·12}$$

The value of L appropriate to a flat plate of breadth b placed edgewise in a wind is (Blasius 1908)

$$L = 1{\cdot}328 \rho^{\frac{1}{2}} \mu^{\frac{1}{2}} Q^{\frac{1}{2}} b^{\frac{1}{2}}. \tag{2·13}$$

If therefore $\mu = \kappa/\sigma$ (2·8) gives

$$\frac{[H]_{\mu=\kappa/\sigma}}{\vartheta_0} = \frac{\kappa}{\mu} \frac{L}{Q} = 1{\cdot}328 \sqrt{(\kappa\rho\sigma Q b)}. \tag{2·14}$$

Making the assumption of Boussinesq and King that $\mu = 0$ it is found that for a flat plate

$$\frac{[H]_{\mu=0}}{\vartheta_0} = \frac{4}{\sqrt{\pi}} \sqrt{(\kappa\rho\sigma Q b)}. \tag{2·15}$$

Hence for a flat plate

$$\frac{[H]_{\mu=\kappa/\sigma}}{[H]_{\mu=0}} = \frac{1{\cdot}328\sqrt{\pi}}{4} = 0{\cdot}589. \tag{2·16}$$

The effect of taking account of the motion in the viscous boundary layer is therefore to reduce the estimate made using Boussinesq's assumption by a factor 0·589. If

Downloaded from https://royalsocietypublishing.org/ on 21 November 2023

the same factor applies to the cooling of cylinders Boussinesq's boundary condition, namely, ϑ = constant at $r = a$, would give

$$\frac{H}{\vartheta_0 \sqrt{(aQ)}} = 4{\cdot}51 \times 0{\cdot}589 \sqrt{(\rho\kappa\sigma)} = 2{\cdot}65 \sqrt{(\rho\kappa\sigma)}, \tag{2·17}$$

and King's boundary condition ($\partial\vartheta/\partial n$ = constant at $r = a$) would give

$$\frac{H}{\vartheta_0 \sqrt{(aQ)}} = 3{\cdot}55 \times 0{\cdot}589 \sqrt{(\rho\kappa\sigma)} = 2{\cdot}09 \sqrt{(\rho\kappa\sigma)}. \tag{2·18}$$

It will be noticed that all these formulae are of the form

$$\frac{H}{\vartheta_0 \sqrt{(aQ)}} = A \sqrt{(\rho\kappa\sigma)}, \tag{2·19}$$

A being a constant. Using the values $\rho = 0{\cdot}00122$, $\kappa = 5{\cdot}0 \times 10^{-5}$, $\sigma = 0{\cdot}2417$, in King's experimental result (2·9), (2·19) is satisfied if $A = 2{\cdot}85$, which is not far from the value 2·65 predicted by taking the temperature of the air at the surface of the cylinder as the same as that of the cylinder and assuming that the reduction in heat transfer due to viscosity is the same as for a flat strip.

If it were true that $\kappa = \mu\sigma$ it would be possible to predict L directly using (2·8) and (2·19) with $A = 2{\cdot}85$, but since one set of measurements of L is available it is better to use the form suggested by (2·19) and determine the value of A which best fits the observations when (2·19) is used in conjunction with (2·8). In the case of a cylinder set obliquely Q must be replaced by $Q \sin i$. Assume therefore

$$\frac{L}{W} = A \frac{\mu}{\kappa} \sqrt{(\rho\kappa\sigma)} \sqrt{(aQ \sin i)}. \tag{2·20}$$

The kinetic theory of gases gives the relationship $\kappa = 1{\cdot}603\mu$, $C_v = 1{\cdot}14\mu\sigma$ for air, and since $W = Q \cos i$, (2·20) can be written in the form

$$L = \tfrac{1}{2} d\rho Q^2 \sqrt{\left(\frac{2}{1{\cdot}14}\right)} A \left(\frac{1}{R}\right)^{\frac{1}{2}} \cos i \sin^{\frac{1}{2}} i \tag{2·21}$$

where $R = dQ\rho/\mu$.

The first step in comparing this formula with Relf & Powell's observation is to divide the value of F_L given in column 3 of table 1 by $\cos i\,(\sin i)^{\frac{1}{2}}$. The results are given in column 6. It will be seen that except for the value at $i = 90°$, which is indeterminate and at $i = 80°$ where the observation is probably inaccurate and at $i = 0$ where they have little meaning, the values are very constant. The values of $F_L/\cos i$ are given in column 7 for comparison with those in column 6. It will be seen that those in column 6 are more constant than those in column 7. The mean value of $F_L(\cos i)^{-1}(\sin i)^{-\frac{1}{2}}$ in column 6 is 0·0036 Lb./ft., so that the value of A which fits the observations is found by inserting in (2·21)

$$0{\cdot}0036 \cos i \sin^{\frac{1}{2}} i \times \frac{453{\cdot}6 \times 981}{30{\cdot}48}$$

instead of L, and

$$d = \tfrac{3}{8} \times 2{\cdot}54, \quad Q = 40 \times 30{\cdot}48, \quad \rho = 0{\cdot}00122,$$

and

$$R = \frac{\frac{3}{8} \times 2{\cdot}54 \times 40 \times 30{\cdot}48 \times 0{\cdot}00122}{1{\cdot}8 \times 10^{-4}} = 7{\cdot}9 \times 10^3.$$

Downloaded from https://royalsocietypublishing.org/ on 21 November 2023

It is found in this way that Relf & Powell's measurements of F_L are closely predicted by (2·21) if A is taken as 4·1 or $A\sqrt{\left(\frac{2}{1\cdot14}\right)} = 5\cdot4$, so that (2·21) becomes

$$L = \tfrac{1}{2}\rho d Q^2 (5\cdot4 R^{-\frac{1}{2}}) \cos i \sin^{\frac{1}{2}} i. \tag{2·22}$$

If A had the value 2·85, deduced by assuming $\kappa = \mu\sigma$ and using King's heat-transfer measurements, the numerical factor in (2·22) would have been 3·78 instead of 5·4. Though for air $a = 1\cdot14\mu\sigma$, it seems hardly likely that this error in the assumptions could account for the difference between 5·4 and 3·78.

It would be of interest to test (2·22) experimentally, particularly at low values of R.

Rough cylinders

If the cylinder is so rough that the boundary layer is not laminar the force cannot be analyzed by the method used for smooth cylinders. In general, it is not possible to make any theory of the aerodynamics of rough cylinders because the force would depend on the exact nature of the roughness. If the roughness consisted of a number of long projections pointing equally in all directions, it is likely that the force on them would be in the direction opposite to that of their motion. The normal component of force N might be divided into portions due to the pressure and to the skin friction, the friction being the resultant force on the projections. In that case the force component formulae might be,

$$\left.\begin{aligned} N &= \tfrac{1}{2}\rho d Q^2 \{[C_D]_p \sin^2 i + C_f \sin i\}, \\ L &= \tfrac{1}{2}\rho d Q^2 C_f \cos i. \end{aligned}\right\} \tag{2·23}$$

This case is illustrated as *b* in figure 2. In the limiting case when the diameter of the cylinder was so small that C_D is negligible compared with C_f the 'cylinder' would look like a hairy string. The force components might then be taken as

$$\left.\begin{aligned} N &= \tfrac{1}{2}\rho d Q^2 C_f \sin i, \\ L &= \tfrac{1}{2}\rho d Q^2 C_f \cos i. \end{aligned}\right\} \tag{2·24}$$

(2·24) might also be expected to apply to a body in the form of a fine thread on which a number of equally spaced spherical beads were threaded. This case is illustrated as *c* in figure 2.

Another possible form of roughness might consist of thin disks or plates set at right angles to a cylinder. In that case the roughness would make a much greater contribution to L than to N, and the appropriate formulae might be

$$\left.\begin{aligned} N &= \tfrac{1}{2}\rho d Q^2 [C_D]_p \sin^2 i, \\ L &= \tfrac{1}{2}\rho d Q^2 C_f \cos i. \end{aligned}\right\} \tag{2·25}$$

This case is illustrated as *d* in figure 2. All these formulae, except those for a smooth cylinder shown as *a* in figure 2, are entirely speculative; they are set down because by using them in an analysis of swimming it might be possible to derive qualitative ideas as to how the nature of the surface of an animal affects its quality as a swimmer.

Downloaded from https://royalsocietypublishing.org/ on 21 November 2023

	$N/\frac{1}{2}\rho d Q^2$	$L/\frac{1}{2}\rho d Q^2$
a	$[C_D]_p \sin^2 i + 4R^{-\frac{1}{2}} \sin^{\frac{3}{2}} i$	$5{\cdot}4R^{-\frac{1}{2}} \cos i \sin^{\frac{1}{2}} i$
b	$[C_D]_p \sin^2 i + C_f \sin i$	$C_f \cos i$
c	$C_f \sin i$	$C_f \cos i$
d	$[C_D]_p \sin^2 i$	$C_f \cos i$

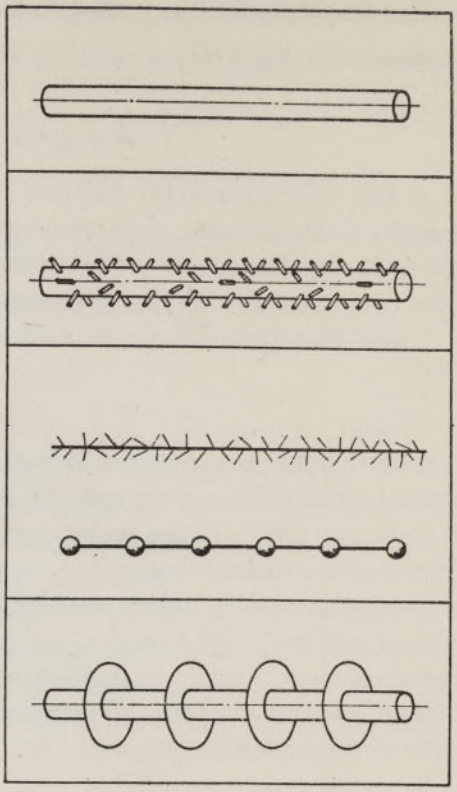

FIGURE 2. Types of roughness with corresponding force formulae.

3. GEOMETRICAL AND KINEMATICAL CONSIDERATIONS AND ASSUMPTIONS

If the backward velocity of the waves relative to the mean position of any material element of the cylinder is U and the velocity with which these waves drive it forwards V, and if the centre line of the cylinder is deformed into a sine curve of amplitude B and wave-length λ, the equation which represents the centre line at time t is

$$y = B \sin \frac{2\pi}{\lambda} \{x + (U - V)\, t\}. \tag{3·1}$$

Here x is the co-ordinate representing distance relative to fixed axes in the direction along which the animal is swimming, y is at right angles to x.

The analysis is simplified by giving the whole field a velocity $U - V$ in the direction $+x$. This reduces the centre line to rest, but each element of the flexible cylinder is now travelling parallel to the centre line with velocity q which is constant if the centre line is assumed to be inextensible. Though, in fact, real animals are by no means inextensible it does not appear that in swimming, as distinct from progressing over solid ground, the centre lines suffer appreciable extension or contraction. The self-propelling property of an inextensible cylinder will be investigated and q will therefore be taken as constant. Figure 3 shows the geometry of the field. Since the fluid is now moving parallel to the axes of x with velocity $U - V$, the angle of incidence of the stream on a *fixed* sine curve would be θ, the angle between the tangent

Downloaded from https://royalsocietypublishing.org/ on 21 November 2023

to the sine curve and the axis of x (see figure 3). Since the particles of the 'snake' are moving along the curve with velocity q, the angle of incidence i, which determines the mechanical reaction of the fluid on an element of the cylinder, is given by

$$\tan i = \frac{(U-V)\sin\theta}{q-(U-V)\cos\theta}, \tag{3·2}$$

and the relative velocity Q is given by

$$Q^2 = q^2 - 2q(U-V)\cos\theta + (U-V)^2. \tag{3·3}$$

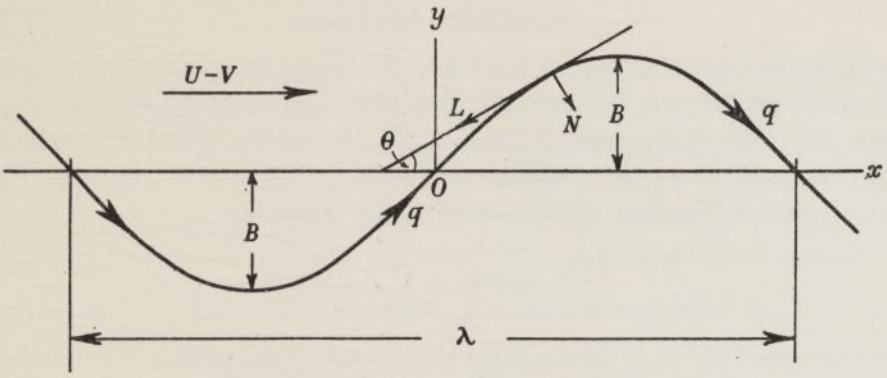

FIGURE 3. Definition of axes.

It is convenient to express these equations in non-dimensional form. Writing

$$V = nU, \quad q = \gamma U, \quad z = \frac{2\pi}{\lambda}\{x+(U-V)t\}, \quad \frac{2\pi B}{\lambda} = \tan\alpha, \tag{3·4}$$

(3·1) becomes

$$\frac{2\pi y}{\lambda} = \tan\alpha \sin z, \tag{3·5}$$

so that

$$\tan\theta\frac{dy}{dx} = \tan\alpha\cos z, \tag{3·6}$$

and

$$\cos\theta = (1+\tan^2\alpha\cos^2 z)^{-\frac{1}{2}}, \quad \sin\theta = \tan\alpha\cos z(1+\tan^2\alpha\cos^2 z)^{-\frac{1}{2}}; \tag{3·7}$$

(3·3) becomes

$$\frac{Q^2}{U^2} = \gamma^2 + (1-n)^2 - 2\gamma(1-n)\cos\theta; \tag{3·8}$$

(3·2) with (3·8) gives

$$\frac{Q}{U}\sin i = (1-n)\sin\theta, \tag{3·9}$$

and

$$\frac{Q}{U}\cos i = \gamma - (1-n)\cos\theta. \tag{3·10}$$

Before going further it may be remarked that γ is a function of α only. Since the velocity U of the waves is defined as the velocity relative to the mean positions of the particles of the animal, the time taken for a wave travelling with velocity U to go one wave-length is equal to the time taken for a particle moving with velocity q along the centre line of the body to traverse one wave-length, so that

$$\gamma = \frac{q}{U} = \frac{\text{length of one wave-length of a sine curve}}{\text{one wave-length}}.$$

Downloaded from https://royalsocietypublishing.org/ on 21 November 2023

Hence $$\gamma = \int_0^\lambda \frac{ds}{\lambda} = \frac{1}{2\pi}\int_0^{2\pi} \frac{dz}{\cos\theta}. \tag{3·11}$$

Substituting for $\cos\theta$ from (3·7) it will be found that

$$\gamma = \frac{2}{\pi}\sec\alpha\, E(\alpha), \tag{3·12}$$

where $E(\alpha)$ is the complete elliptic integral of the second kind. This has been tabulated for value of α between 0 and $\frac{1}{2}\pi$.

Equilibrium conditions

It will be assumed that the animal forms itself into an integral number of wavelengths. The equilibrium condition is then that the resultant force on one wavelength is zero. The component of force in the direction y is certainly zero because the symmetry of the assumed shape ensures that this shall be the case. The equilibrium condition therefore resolves itself in the equation

$$\int_0^\lambda N\sin\theta\, ds = \int_0^\lambda L\cos\theta\, ds. \tag{3·13}$$

Further progress can only be made by substituting expressions like those given in §2 to represent N and L in terms of Q and i. If one of these be selected and Q and i given their values in terms of z using (3·3), (3·7), (3·9) and (3·10), the equilibrium equation (3·13) is then expressed as a relation between definite integrals. For any given value of α and n these can be integrated numerically, and a relation between α, n and the experimentally determined constants contained in the expressions for N and L can be found. The two types of expression (2·3) and (2·22) appropriate to smooth animals and (2·23), (2·24) or (2·25) for rough animals will next be discussed separately.

4. Smooth animals

The expressions (2·3) and (2·22) developed in §2 for the components of force on a smooth cylinder contain $R = Qd\rho/\mu$. In discussing the swimming characteristics of any waving movement the animal may make, it is more convenient to define the Reynolds number in terms of velocity U which is the same for all parts of the body. Thus if

$$R_1 = Ud\rho/\mu, \tag{4·1}$$

from (3·8) $$R = R_1\{\gamma^2 + (1-n)^2 - 2\gamma(1-n)\cos\theta\}^{\frac{1}{2}}; \tag{4·2}$$

substituting for R, Q and i in (2·3) and (2·22)

$$N = \tfrac{1}{2}\rho dU^2\{[C_D]_p\,(1-n)^2\sin^2\theta + 4R_1^{-\frac{1}{2}}(1-n)^{\frac{3}{2}}\sin^{\frac{3}{2}}\theta\} \tag{4·3}$$

and $$L = \tfrac{1}{2}\rho dU^2\{5{\cdot}4(1-n)^{\frac{1}{2}}R_1^{-\frac{1}{2}}\sin^{\frac{1}{2}}\theta[\gamma - (1-n)\cos\theta]\}. \tag{4·4}$$

At this stage it is necessary to point out that θ may be positive or negative. The first term in the expression (4·3) for N contains $\sin^2\theta$ as a factor, but the direction of the normal force is reversed when θ changes sign. For this reason when the expression for N is inserted in (4·3), $(\sin\theta)\,|\sin\theta|$ should be written instead of

Downloaded from https://royalsocietypublishing.org/ on 21 November 2023

$\sin^2\theta$, but if the limits in the integrals (3·13) are taken as 0 and $\frac{1}{4}\lambda$ instead of 0 and λ, θ does not change sign and symmetry ensures that the resulting equation is true if (4·3) is true. After inserting (4·3) and (4·4) in (3·13), the equilibrium is found to be

$$[C_D]_p R_1^{\frac{1}{2}} C = 5{\cdot}4\gamma(1-n)^{-\frac{1}{2}}\frac{2}{\pi}\int_0^{\frac{1}{2}\pi}\sin^{\frac{1}{2}}\theta\,dz$$

$$-(1-n)^{-\frac{1}{2}}\frac{2}{\pi}\left\{5{\cdot}4\int_0^{\frac{1}{2}\pi}\sin^{\frac{1}{2}}\theta\cos\theta\,dz+4\int_0^{\frac{1}{2}\pi}\sin^{\frac{1}{2}}\theta\sec\theta\,dz\right\}, \quad (4{\cdot}5)$$

where

$$C=\frac{2}{\pi}\int_0^{\frac{1}{2}\pi}\frac{\sin^3\theta}{\cos\theta}\,dz. \quad (4{\cdot}6)$$

When the expressions (3·7) for $\sin\theta$ and $\cos\theta$ are inserted in (4·5) the integrals are intractable but they can be integrated numerically. For this purpose a value of α was first fixed. (3·7) was then used to find the values of $\cos\theta$ and $\sin\theta$ corresponding with the ten values of z which divide 90° into nine equal parts. When integrating, the values of the integrands at $z=0$ and $z=\frac{1}{2}\pi$ were halved and added to the sum of the other eight values. The result was divided by 9. This gives an approximation to the value of $\frac{2}{\pi}\int_0^{\frac{1}{2}\pi}$ (integrand) dz which is accurate enough for the present work.

Values of

$$I_1=\frac{2}{\pi}\int_0^{\frac{1}{2}\pi}\sin^{\frac{1}{2}}\theta\,dz,\quad I_2=\frac{2}{\pi}\int_0^{\frac{1}{2}\pi}\sin^{\frac{1}{2}}\theta\cos\theta\,dz,$$

$$I_3=\frac{2}{\pi}\int_0^{\frac{1}{2}\pi}\sin^{\frac{1}{2}}\theta\sec\theta\,dz,\quad I_4=\frac{2}{\pi}\int_0^{\frac{1}{2}\pi}\sin^{\frac{1}{2}}\theta\sec\theta\,dz$$

obtained in this way are given in table 3.

TABLE 3

α	I_1	I_2	I_3	I_4
0	0	0	0	0
10	0·315	0·312	0·006	0·318
20	0·446	0·429	0·034	0·463
30	0·547	0·501	0·098	0·599
40	0·633	0·537	0·213	0·750
50	0·711	0·542	0·413	0·954
60	0·782	0·505	0·762	1·267
70	0·849	0·424	1·450	1·873
80	0·910	0·276	3·388	3·603
90	1·000	0	∞	∞

When the expressions (3·7) for $\cos\theta$ are substituted in (4·6) the integral C can be expressed explicitly as a function of α. In fact

$$C=\frac{2}{\pi}[\tan\alpha-\cos\alpha\log\tan(\tfrac{1}{4}\pi+\tfrac{1}{2}\alpha)]. \quad (4{\cdot}7)$$

Values of C and γ and $\frac{B}{\lambda}=\frac{1}{2\pi}\tan\alpha$ are given in columns 2, 3 and 4 of table 4. Values of $[C_D]_p R_1^{\frac{1}{2}}$ obtained by inserting these values in (4·5) are given in table 5.

Downloaded from https://royalsocietypublishing.org/ on 21 November 2023

The results of these calculations can conveniently be displayed in a diagram which may be called a 'swimming diagram' in which contours of equal values of $[C_D]_p R_1^{\frac{1}{2}}$ are shown, the ordinates representing $n = V/U$ and the abscissae, α. To produce such a diagram it is necessary to interpolate between the calculated values

TABLE 4

$\alpha°$	B/λ	γ	C	A_1	A_2	A_3	A_4	A_5	A_6
0	0	1·0000	0	1·0000	1·0000	1·0000	1·0000	1·0000	1·0000
5	0·0139	1·0019	0·0004	0·9981	0·9962	0·9943	0·9924	0·9905	0·9887
10	0·0281	1·0077	0·0022	0·9923	0·9848	0·9773	0·9699	0·8626	0·9560
15	0·0426	1·0178	0·0077	0·9827	0·9659	0·9518	0·9335	0·9216	0·9028
20	0·0579	1·0324	0·0185	0·9691	0·9397	0·9116	0·8847	0·8591	0·8346
25	0·0742	1·0523	0·0367	0·9514	0·9063	0·8644	0·8256	0·7894	0·7553
30	0·0919	1·0788	0·0647	0·9294	0·8660	0·8071	0·7577	0·7097	0·6698
35	0·1114	1·1132	0·1053	0·9029	0·8192	0·7471	0·7254	0·6329	0·5829
40	0·1335	1·1577	0·1558	0·8713	0·7660	0·6793	0·6077	0·5524	0·4985
45	0·1592	1·2160	0·2398	0·8347	0·7071	0·6080	0·5303	0·4689	0·4198
50	0·1897	1·2930	0·3452	0·7921	0·6428	0·5239	0·4520	0·3839	0·3486
55	0·2273	1·3970	0·4877	0·7430	0·5736	0·4598	0·3812	0·3277	0·2856
60	0·2757	1·5420	0·6835	0·6864	0·5000	0·3856	0·3125	0·2641	0·2305
65	0·3413	1·7531	0·9600	0·6211	0·4226	0·3132	0·2490	0·2092	0·1824
70	0·4373	2·0817	1·3713	0·5453	0·3420	0·2437	0·1910	0·1602	0·1400
75	0·5940	2·6476	2·0418	0·4561	0·2588	0·1826	0·1385	0·1197	0·1018
80	0·9026	3·8133	3·3410	0·3485	0·1736	0·1152	0·0894	0·0756	0·0664
85	1·8191	7·3732	7·1028	0·2127	0·0872	0·0567	0·0439	0·0377	0·0329
90	—	—	—	0	0	0	0	0	0

TABLE 5. SMOOTH ANIMALS: VALUES OF $[C_D]_p R_1^{\frac{1}{2}}$

n \ α	20°	20°	30°	40°	50°	60°	70°	80°
0·95	—	—	—	—	—	—	—	482
0·9	$2·2 \times 10^4$	$3·8 \times 10^3$	$1·4 \times 10^3$	713	413	274	201	163
0·8	$6·9 \times 10^3$	1200	444	226	131	87·6	64·6	52·6
0·7	$3·3 \times 10^3$	603	213	109	63·5	42·7	31·6	25·9
0·6	1820	321	119	61·1	35·9	24·3	18·2	15·0
0·5	1083	192	71·6	37·0	21·9	15·0	11·4	9·50
0·4	655	118	44·2	23·1	13·80	9·60	7·37	6·26
0·3	384	71·0	26·9	14·3	8·70	6·17	4·84	4·19
0·2	204	39·5	15·3	8·38	5·26	3·87	3·13	2·80
0·1	78·4	17·6	7·25	4·27	2·86	2·26	1·94	1·82
0	—	1·82	1·41	1·28	1·12	1·08	1·06	1·11
−0·1	—	—	—	—	—	0·20	0·41	0·56
−0·2	—	—	—	—	—	—	—	0·16

given in table 5. The resulting diagram is shown in figure 4. Since the angle α is not directly measurable on photographs of swimming animals, the scale for $\frac{B}{\lambda} = \frac{1}{2\pi}\tan\alpha$ is marked on the top of the diagram. Limitations to the application of this analysis are discussed in §9.

Downloaded from https://royalsocietypublishing.org/ on 21 November 2023

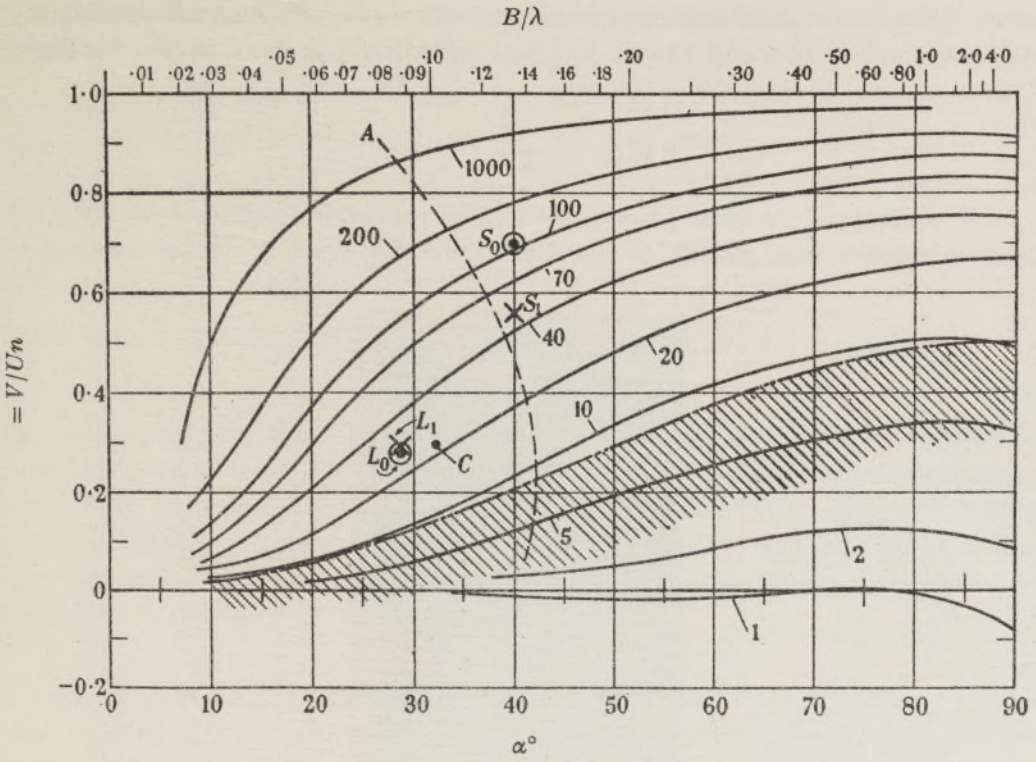

FIGURE 4. Swimming diagram for long, smooth animals showing contours for constant values of $[C_D]_p R_1^{\frac{1}{2}}$. Line A represents conditions for maximum speed with given energy output.

5. COMPARISON WITH PHOTOGRAPHS OF SWIMMING SNAKE AND LEECH

Snake

Figure 5 shows a sequence of photographs of a snake taken at intervals of $\frac{1}{16}$ s by Professor James Gray. The snake is swimming in a shallow trough over a grid of 5 cm squares. Each photograph is displaced two squares downwards from its predecessor. It will be seen that the waves increase as they pass from head to tail. To measure V and U the centre lines of the snake in each position were traced and the results superposed to form the diagram of figure 6. The position of the head in each case is shown as a black dot; the broken line AB in figure 6 is drawn so that it passes closely along the path pursued by the head. It will be seen that the head only deviates slightly from this line, but that the tail moves violently. Using figure 6 Gray found that the head moves 10 cm in $\frac{5}{16}$ s, so that $V = 32$ cm/s. To measure U is not easy, partly because the amplitude of the motion is not constant. The velocities of the maxima (i.e. the points on the curves furthest from the broken line AB in figure 6) were measured. The maximum marked D in figure 6 appears in all the frames. During the $\frac{5}{16}$ s interval between frame 1 and frame 6 it moved back 4·5 cm. The maximum marked C is pronounced only between frames 3 and 6. During the corresponding interval of $\frac{3}{16}$ s it moved back 1·8 cm. The maximum marked E exists between frames 1 and 4. During the corresponding $\frac{3}{16}$ s it moves

Downloaded from https://royalsocietypublishing.org/ on 21 November 2023

3·4 cm. The wave velocities corresponding with the maxima C, D and E respectively are therefore 9·6, 14·5 and 18·0 cm/s. These velocities are equal to $U - V$. Their mean is 14 cm/s, so that if $V = 32$ cm/s

$$n = \frac{V}{U} = \frac{32}{32+14} = 0{\cdot}7. \tag{5·1}$$

A rough estimate of the mean amplitude of the waves can be obtained by finding the distance between lines parallel to the broken line AB which touch the maxima at

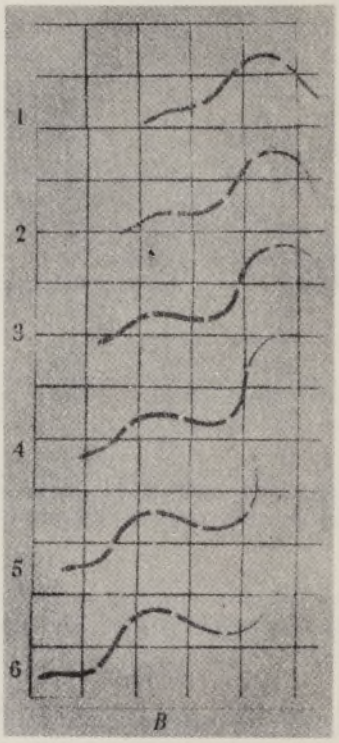

FIGURE 5. Snake (*Natrix*) swimming in water; 5 cm squares, 16 frames per second (J. Gray).

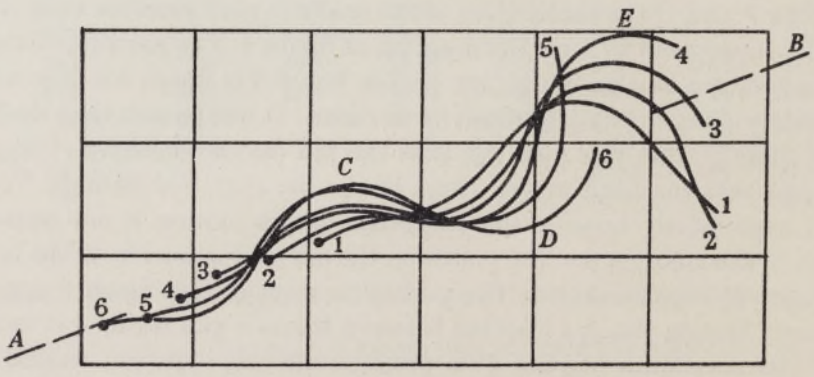

FIGURE 6. Centre lines of snake superposed. AB, mean line of motion of head; C, D, E, maximum distances from AB.

Downloaded from https://royalsocietypublishing.org/ on 21 November 2023

D and E. In the case of frame 6 this is $2B = 4{\cdot}7$ cm, and the corresponding wavelength is 17·6 cm. So that

$$B/\lambda = 0{\cdot}134. \tag{5·2}$$

The point corresponding with $n = 0{\cdot}7$, $B/\lambda = 0{\cdot}134$ is marked in figure 4 at S_0. It will be seen that it falls near the line $[C_D]_p R_1^{\frac{1}{2}} = 100$. The diameter of cross-section of the snake as measured on the photographs was 0·6 cm. The velocity U was $32 + 14 = 46$ cm/s and for water $\mu = 0{\cdot}011$, so that

$$R_1 = \frac{46 \times 0{\cdot}6}{0{\cdot}011} = 2500.$$

It has been seen in §2 that $[C_D]_p$ is approximately 1·0, so that

$$[C_D]_p R_1^{\frac{1}{2}} = (2500)^{\frac{1}{2}} = 50. \tag{5·3}$$

The point where the line $[C_D]_p R_1^{\frac{1}{2}} = 50$ cuts the abscissa $B/\lambda = 0{\cdot}134$ is shown as a cross at S_1 in figure 4. This corresponds to $V/U = 0{\cdot}55$. The swimming efficiency which may be judged by the value of U/V is therefore rather larger than that predicted assuming a wave of constant amplitude, but the fact that the measurements of B/λ and of V/U vary over such a wide range would make accurate prediction impossible.

Leech

Figure 7 shows eight successive frames in a sequence of photographs of a large leech swimming from right to left over a grid of 2 cm squares. The frequency of the photographs is 15/s. It was found that the average speed of the head forward was 2·0 cm in seven frames so that $V = 2 \times \frac{15}{7} = 4{\cdot}3$ cm/s. The velocity backwards of the crests and troughs of the waves were obtained by measuring the slopes of the broken lines drawn through them in figure 7. The velocity backwards of the first wave corresponding with the crest which extends from frame 1 to frame 6 is $U - V = 12$ cm/s, that corresponding with the first trough extending from frame 3 to frame 8 is also 12 cm/s. The velocity of the second crest extending from frame 5 to frame 8 is 7·5 cm/s, so that if the first crest and first trough which each appear on six frames are used $U = 12 + 4{\cdot}3 = 16{\cdot}3$ cm/s, while the last crest which appears only in the four frames 5 to 8 give $U = 7{\cdot}5 + 4{\cdot}3 = 11{\cdot}8$ cm/s. Perhaps the best way to weight these observations is to take

$$U = \frac{5 \times 16{\cdot}3 + 5 \times 16{\cdot}3 + 3 \times 11{\cdot}8}{13} = 15{\cdot}3 \text{ cm/s},$$

so that

$$n = \frac{V}{U} = \frac{4{\cdot}3}{15{\cdot}3} = 0{\cdot}28. \tag{5·4}$$

To obtain a mean value for B/λ a tangent line was drawn wherever possible to touch the curved profile at two points, and the maximum distance of the body of the leech from this line was measured in each frame. This distance was taken as $2B$ and the distance between the points of contact as λ; in this way the following values of B/λ were obtained: 0·06, 0·07, 0·09, 0·09, 0·08, 0·16, 0·07. The mean value is

$$B/\lambda = 0{\cdot}089. \tag{5·5}$$

The point $V/U = 0{\cdot}28$, $B/\lambda = 0{\cdot}089$ is marked as L_0 in figure 4. It will be seen that it lies between the contours $[C_D]_p R_1^{\frac{1}{2}} = 20$ and $[C_D]_p R_1^{\frac{1}{2}} = 40$.

Downloaded from https://royalsocietypublishing.org/ on 21 November 2023

Unfortunately, the leech is not circular in section but approximately elliptical; in fact, the dimensions of the axes or the ellipse as seen in figure 7 are 0·2 and 0·9 cm. Taking d as the mean of these,

$$d = 0{\cdot}55\,\text{cm},$$

so that

$$R_1 = \frac{0{\cdot}55 \times 15{\cdot}3}{0{\cdot}011} = 770.$$

Taking $[C_D]_p$ as 1·0 this gives

$$[C_D]_p R_1^{\frac{1}{2}} = 28. \tag{5·6}$$

The point L_1 in figure 4 corresponds with the value of V/U predicted by the diagram.

It will be seen therefore that the swimming performance of the leech is close to what would be expected if it were a smooth cylinder.

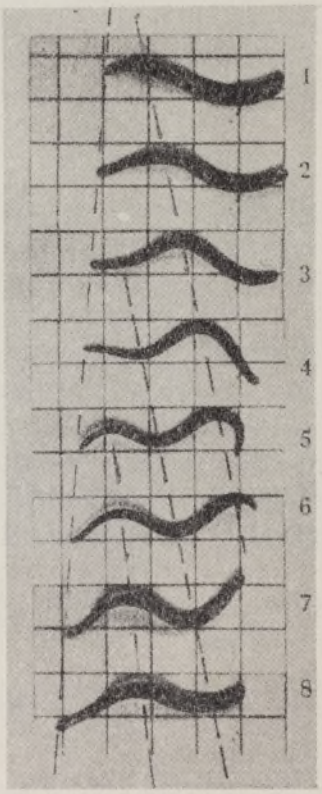

FIGURE 7. Leech swimming in water; 2 cm squares, 15 frames per second (J. Gray).

6. ENERGY REQUIRED FOR PROPULSION OF SMOOTH ANIMALS

The rate, W, at which the animal does work on the surrounding fluid per unit length of its body is the mean value of

$$N(U-V)\sin\theta + L\{q-(U-V)\cos\theta\}$$

or

$$U(1-n)\{N\sin\theta - L\cos\theta\} + qL. \tag{6·1}$$

Downloaded from https://royalsocietypublishing.org/ on 21 November 2023

The first term in (6·1) vanishes owing to the equilibrium condition (3·13) so that from (4·4)

$$W = q \times (\text{mean value of } L)$$
$$= \tfrac{1}{2}\rho d(5{\cdot}4\gamma U^3 R_1^{-\frac{1}{2}})(1-n)^{-\frac{1}{2}}\frac{2}{\pi}\int_0^{\frac{1}{2}\pi}\{\gamma-(1-n)\cos\theta\}\sin^{\frac{1}{2}}\theta\sec\theta\,\mathrm{d}z. \quad (6{\cdot}2)$$

It is of interest to know the amplitude of wave which would propel the animal at a given speed with the least output of energy. For this reason it is useful to express (6·2) in terms of V rather than U. Remembering that R_1 contains U as a factor, the required expression is

$$W = \frac{5{\cdot}4}{2}\rho d V^3\left(\frac{\mu}{\rho d V}\right)^{\frac{1}{2}} G(n,\alpha), \quad (6{\cdot}3)$$

where
$$G(n,\alpha) = (1-n)^{\frac{1}{2}} n^{-\frac{1}{2}}\{(\gamma^2-\gamma)I_4 + n\gamma I_1\} \quad (6{\cdot}4)$$

and
$$I_4 = \frac{2}{\pi}\int_0^{\frac{1}{2}\pi}\sin^{\frac{1}{2}}\theta\sec\theta\,\mathrm{d}z, \quad I_1 = \frac{2}{\pi}\int_0^{\frac{1}{2}\pi}\sin^{\frac{1}{2}}\theta\,\mathrm{d}z. \quad (6{\cdot}5)$$

Values of I_1 and I_4 are given in table 3 and values of $G(n\alpha)$ are given in table 6. Using auxiliary diagrams it is possible to construct from the figures of table 6 a diagram analogous to figure 4 which displays lines of constant $G(n,\alpha)$ on a diagram (figure 8) whose ordinates are n and abscissae α.

TABLE 6. VALUES OF $G(n,\alpha)$

α° \ n	0·1	0·2	0·3	0·4	0·5	0·6	0·7	0·8	0·9
0	—	—	—	—	—	—	—	—	—
10	11·2	3·44	1·80	1·01	0·66	0·44	0·30	0·20	0·12
20	23·8	6·27	2·91	1·66	1·05	0·70	0·47	0·31	0·18
30	49·6	11·2	4·81	2·62	1·61	1·04	0·69	0·45	0·26
40	104	20·1	8·37	4·33	2·56	1·62	1·05	0·67	0·38
50	212	43·0	16·1	7·98	4·54	2·78	1·76	1·10	0·62
60	578	102	36·8	17·5	9·64	5·74	3·54	2·16	1·19
70	1957	335	117	54·0	28·0	16·8	10·1	6·06	3·27
80	14780	2481	848	385	203	116	68·6	40·4	21·4

Wave for minimum output of energy

The lines displayed in figure 8 correspond with conditions under which constant energy output is required to propel an animal at a given speed. By superposing the diagram on that of figure 4 which displays lines of constant $[C_D]_p R_1^{\frac{1}{2}}$ a set of possible values of R_1 are obtained, but since for a constant V and d, R_1 is not constant, this superposition has little meaning. To find the minimum value of W corresponding with any given value of d and V it is necessary to construct a diagram similar to figure 4 but displaying contours of constant $[C_D]_p\left(\frac{dV\rho}{\mu}\right)^{\frac{1}{2}}$. That is to say, the values of $[C_D]_p R_1^{\frac{1}{2}}$ given in table 5 must be multiplied by $n^{\frac{1}{2}}$ to give the figures of table 7 and a new set of contours drawn. The diagram obtained in this way is shown in figure 9. It will be seen that its curves are similar in general appearance to those of figure 4.

Downloaded from https://royalsocietypublishing.org/ on 21 November 2023

The set of values of α and n which characterize the propulsion of the animal at a given value of V are found by moving along the appropriate contour in figure 9.

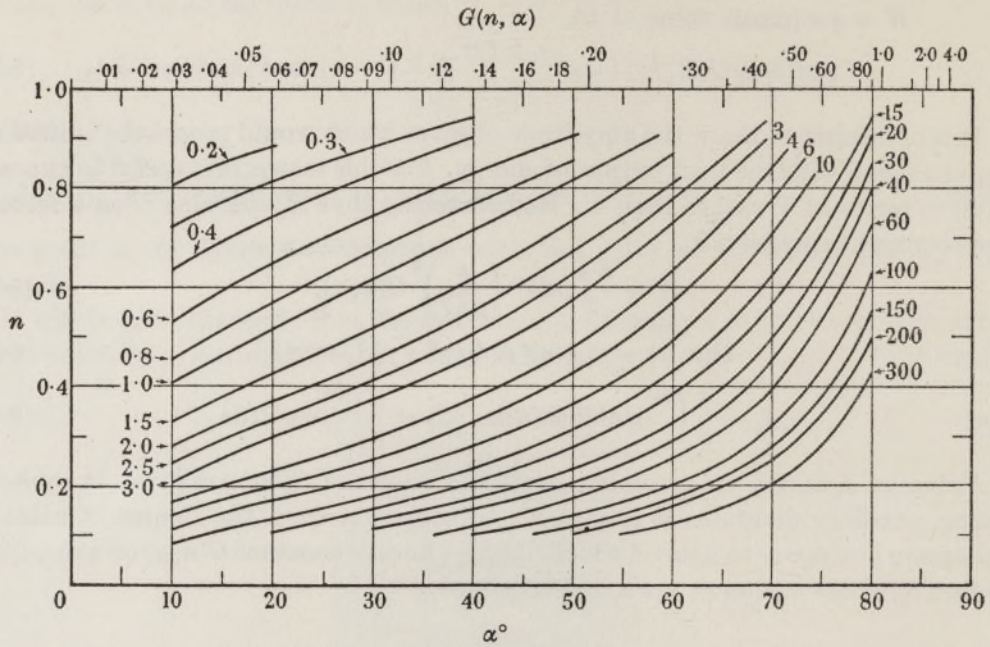

FIGURE 8. $G(n, \alpha)$. Shows in non-dimensional form the rate of dissipation of energy.

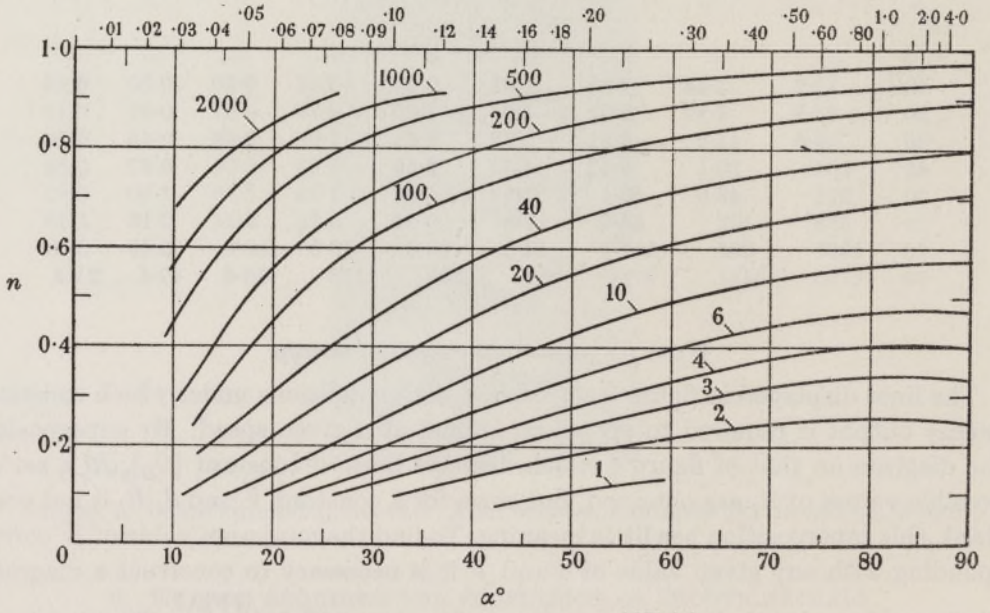

FIGURE 9. Contours of $[C_D]_p \left(\frac{dV\rho}{\mu}\right)^{\frac{1}{2}}$.

To find the particular value of α which corresponds with the least energy output, figure 8 may be superposed on figure 9. The required value of α will be that corresponding with the point on the contour of $[C_D]_p \left(\frac{dV\rho}{\mu}\right)^{\frac{1}{2}}$, where it touches one of the

Downloaded from https://royalsocietypublishing.org/ on 21 November 2023

TABLE 7. VALUES OF $[C_D]_p \left(\frac{dV\rho}{\mu}\right)^{\frac{1}{2}}$

α° \ n	0·1	0·2	0·3	0·4	0·5	0·6	0·7	0·8	0·9
10	24·8	91·1	210	414	766	1415	2757	6203	20968
20	5·57	17·7	38·9	74·6	136	249	504	1079	3632
30	2·29	6·85	14·7	28·0	50·6	92·2	178	397	1280
40	1·35	3·75	7·83	14·6	21·2	47·3	90·8	202	676
50	0·90	2·35	4·77	8·75	15·5	27·8	53·1	117	392
60	0·71	1·73	3·38	6·07	10·6	18·8	35·7	78·3	260
70	0·61	1·40	2·65	4·66	8·03	14·1	26·4	57·8	191
80	0·58	1·25	2·30	3·96	6·71	11·7	21·7	47·1	154

superposed contours of $G(n, \alpha)$. In this way the points on the broken line shown as *A* in figure 4, were found. Though there is no physical reason to suppose that animals do in fact swim by forming the particular type of wave which involves least output of energy, it is worth noticing that the point in figure 4 which corresponds to a swimming snake is close to this line. The point corresponding with a swimming leech is well to the left of the line, showing that this specimen bent its body rather less than would be expected if the most efficient movement were used.

7. SWIMMING OF A ROUGH FLEXIBLE CYLINDER

Similar analysis to that applied to a smooth swimmer can be applied to one with a rough surface, using any of the force-component formulae discussed in § 2. When the geometrical relationships (3·2), (3·9), (3·10) giving i and Q as functions of U, θ, n and α are inserted, the force components appropriate to the cases *b*, *c*, *d* of figure 2 are

$$(b)\quad \frac{N}{\frac{1}{2}\rho d U^2} = [C_D]_p (1-n)^2 \sin^2\theta + C_f(1-n)\sin\theta\{\gamma^2+(1-n)^2-2\gamma(1-n)\cos\theta\}^{\frac{1}{2}} \quad (7{\cdot}1)$$

$$\frac{L}{\frac{1}{2}\rho d U^2} = C_f\{\gamma-(1-n)\cos\theta\}\{\gamma^2+(1-n)^2-2\gamma(1-n)\cos\theta\}^{\frac{1}{2}}; \quad (7{\cdot}2)$$

(*c*) is obtained from (*b*) by setting $[C_D]_p = 0$ and for (*d*)

$$\frac{N}{\frac{1}{2}\rho d U^2} = [C_D]_p (1-n)^2 \sin^2\theta, \quad (7{\cdot}3)$$

$$\frac{L}{\frac{1}{2}\rho d U^2} = C_f\{\gamma-(1-n)\cos\theta\}\{\gamma^2+(1-n)^2-2\gamma(1-n)\cos\theta\}^{\frac{1}{2}}. \quad (7{\cdot}4)$$

Substituting for L and N in the equation of equilibrium (3·13) a relationship between $[C_D]_p/C_f$ and n, γ and α is obtained in each case. These are

$$(b)\quad \frac{[C_D]_p}{C_f}(1-n)^2 C = \frac{2}{\pi}\int_0^{\frac{1}{2}\pi}\{\gamma-(1-n)\sec\theta\}\{\gamma^2+(1-n)^2-2\gamma(1-n)\cos\theta\}^{\frac{1}{2}}\,dz, \quad (7{\cdot}5)$$

$$(d)\quad \frac{[C_D]_p}{C_f}(1-n)^2 C = \frac{2}{\pi}\int_0^{\frac{1}{2}\pi}\{\gamma-(1-n)\cos\theta\}\{\gamma^2+(1-n)^2-2\gamma(1-n)\cos\theta\}^{\frac{1}{2}}\,dz, \quad (7{\cdot}6)$$

$$(c)\quad \int_0^{\frac{1}{2}\pi}\{\gamma(1-n)\sec\theta\}\{\gamma^2+(1-n)^2-2\gamma(1-n)\cos\theta\}^{\frac{1}{2}}\,dz = 0. \quad (7{\cdot}7)$$

Downloaded from https://royalsocietypublishing.org/ on 21 November 2023

The occurrence of $\sec\theta$ in (7·5) arises because the last term

$$C_f(1-n)\sin\theta\{\gamma^2+(1-n)^2-2\gamma(1-n)\cos\theta\}^{\frac{1}{2}}$$

in (7·1) is multiplied by $\sin\theta\,dz/\cos\theta$ and transferred to the right-hand side of (7·5), where $\sin^2\theta/\cos\theta$ combines with $\cos\theta$ to produce $\sec\theta$. Here C has the same meaning as in (4·6).

To integrate (7·5) and (7·6) numerically the method adopted in the case of smooth cylinders may be used. As an alternative the integrands can be expanded in powers of $\cos\theta$:

$$\{\gamma^2+(1-n)^2-2\gamma(1-n)\cos\theta\}^{\frac{1}{2}}$$
$$=\{\gamma^2+(1-n)^2\}^{\frac{1}{2}}\Big\{1-\tfrac{1}{2}m\cos\theta-\tfrac{1}{8}m^2\cos^2\theta-\tfrac{1}{16}m^3\cos^3\theta$$
$$-\frac{5}{2^7}m^4\cos^4\theta-\frac{7}{2^8}m^5\cos^5\theta-\frac{21}{2^{10}}m^6\cos^6\theta\ldots\Big\},\qquad(7\cdot8)$$

where
$$m=\frac{2\gamma(1-n)}{\gamma^2+(1-n)^2}.\qquad(7\cdot9)$$

Writing
$$A_n=\frac{2}{\pi}\int_0^{\frac{1}{2}\pi}\cos^n\theta\,dz=\int_0^{\frac{1}{2}\pi}(1+\tan^2\alpha\cos^2 z)^{-\frac{1}{2}n}\,dz,\qquad(7\cdot10)$$

$$\frac{2}{\pi}\int_0^{\frac{1}{2}\pi}\{\gamma-(1-n)\sec\theta\}\{\gamma^2+(1-n)^2-2\gamma(1-n)\cos\theta\}^{\frac{1}{2}}\,dz$$
$$=\{\gamma^2+(1-n)^2\}^{\frac{1}{2}}\Big\{-(1-n)A_{-1}+[\tfrac{1}{2}m(1-n)+\gamma]A_0-[\tfrac{1}{2}m\gamma-\tfrac{1}{8}m^2(1-n)]A_1$$
$$-[\tfrac{1}{8}m^2\gamma-\tfrac{1}{16}m^3(1-n)]A_2-\Big[\tfrac{1}{16}m^3\gamma-\frac{5}{2^7}m^4(1-n)\Big]A_3-\Big[\frac{5}{2^7}m^4\gamma-\frac{7}{2^8}m^5(1-n)\Big]A_4$$
$$-\Big[\frac{7}{2^8}m^5\gamma-\frac{21}{2^{10}}m^6(1-n)\Big]A_5-\Big[\frac{21}{2^{10}}m^6\gamma-\frac{33}{2^{11}}m^7(1-n)\Big]A_6-\ldots\Big\}\qquad(7\cdot11)$$

and

$$\frac{2}{\pi}\int_0^{\frac{1}{2}\pi}\{\gamma-(1-n)\cos\theta\}\{\gamma^2+(1-n)^2-2\gamma(1-n)\cos\theta\}^{\frac{1}{2}}\,dz$$
$$=\{\gamma^2+(1-n)^2\}^{\frac{1}{2}}\Big\{\gamma-[\tfrac{1}{2}m\gamma+1-n]A_1+[\tfrac{1}{2}m(1-n)-\tfrac{1}{8}\gamma m^2]A_2$$
$$+[\tfrac{1}{8}m^2(1-n)-\tfrac{1}{16}m^3\gamma]A_3+\Big[\tfrac{1}{16}m^3(1-n)-\frac{5}{2^7}m^4\gamma\Big]A_4+\ldots\Big\}\qquad(7\cdot12)$$

Expressions for the integrals A_n can be derived from recurrence formula

$$\frac{d}{d\alpha}(A_n)=\frac{2}{\pi}\int_0^{\frac{1}{2}\pi}\frac{d}{d\alpha}(1+\tan^2\alpha\cos^2 z)^{-\frac{1}{2}n}\,dz$$
$$=-n\cot\alpha\sec^2\alpha(A_n-A_{n+2}),$$

so that
$$A_{n+2}=A_n-\frac{1}{n}\cos\alpha\sin\alpha A_n',\qquad(7\cdot13)$$

Downloaded from https://royalsocietypublishing.org/ on 21 November 2023

where A_n' is written for $\frac{\mathrm{d}}{\mathrm{d}\alpha} A_n$. The expressions for A_3, A_4, A_5 and A_6 given in Table 8 were obtained from A_1 and A_2, using (7·13). Here K is the complete elliptic integral of the first kind, namely

$$K = \int_0^{\frac{1}{2}\pi} \frac{\mathrm{d}z}{(1-\sin^2\alpha\sin^2 z)^{\frac{1}{2}}}, \tag{7·14}$$

and K' and K'' are $\frac{\mathrm{d}}{\mathrm{d}\alpha} K$ and $\frac{\mathrm{d}^2}{\mathrm{d}\alpha^2} K$.

Table 4 gives values of A_1 to A_6; B/λ, γ and C are also given.

The results of calculations can be displayed in a swimming diagram like that of figure 4, but the quantity $[C_D]_p R_1^{\frac{1}{2}}$, the values of which were shown in figure 4, is replaced by $[C_D]_p/C_f$. The results for the type of roughness shown diagrammatically as (*d*) in figure 2 are shown in figure 10. The contours of equal values of $[C_D]_p/C_f$ shown in figure 10 differ from those for smooth cylinders, figure 4, in that negative values of V/U occur in a part of the diagram which might correspond with physically possible circumstances. This cannot be said of figure 4.

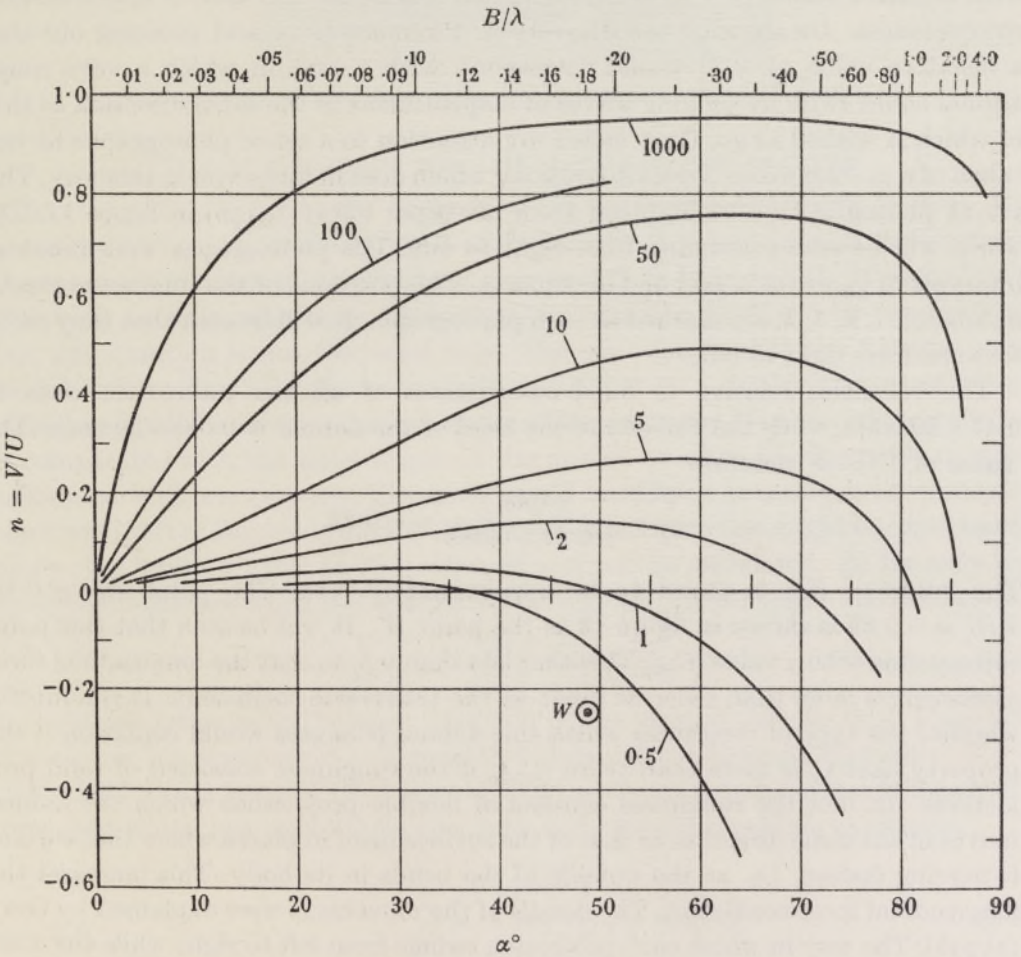

FIGURE 10. Swimming diagram for rough cylinder. Values of $[C_D]_p/C_f$.

Downloaded from https://royalsocietypublishing.org/ on 21 November 2023

TABLE 8

$$A_{-1} = \frac{2}{\pi}\int_0^{\frac{1}{2}\pi} \sec\theta\, dz = \frac{2}{\pi}\sec\alpha E(\alpha) = \gamma$$

$$A_0 = 1$$

$$A_1 = \frac{2}{\pi}\cos\alpha\, K(\alpha)$$

$$A_2 = \frac{2}{\pi}\int_0^{\frac{1}{2}\pi} (1+\tan^2\alpha\cos^2 z)\, dz = \cos\alpha$$

$$A_3 = \frac{2}{\pi}[K(\alpha)\cos^3\alpha + K'(\alpha)\cos^2\alpha\sin\alpha]$$

$$A_4 = \tfrac{7}{8}\cos\alpha + \tfrac{1}{8}\cos 3\alpha$$

$$A_5 = A_3 - \frac{2}{\pi}\{\tfrac{1}{8}[K(\alpha) - \tfrac{1}{3}K''(\alpha)](\cos\alpha - \tfrac{1}{2}\cos 3\alpha - \tfrac{1}{2}\cos 5\alpha) - \tfrac{1}{12}K'(\alpha)(\sin 3\alpha + \sin 5\alpha)\}$$

$$A_6 = A_4 - \tfrac{5}{64}\cos\alpha + \tfrac{7}{128}\cos 3\alpha + \tfrac{3}{128}\cos 5\alpha$$

8. THE SWIMMING OF THE MARINE WORM *NEREIS DIVERSICOLOR*

In preparing the diagram shown in figure 10 the parts of the curves corresponding with negative values of V/U were calculated merely for the sake of mathematical completeness. On showing the diagram to Professor Gray and pointing out that a negative value of V/U would correspond with a case in which a very rough animal could swim by sending waves of displacement in the same direction as that in which it wished to go, Gray called my attention to a set of photographs he had taken of a marine worm *Nereis diversicolor* which does in fact swim in this way. This set of photographs is reproduced from his paper (Gray 1939*b*) in figure 11. The worm will be seen swimming from right to left. The photographs were taken at intervals of $\frac{1}{20}$ s over a grid of 1 in. squares. The positions of the four wave crests, numbered 1, 2, 3, 4, are marked in each photograph. It will be seen that they move forward from right to left.

The velocities relative to fixed co-ordinates of all the waves are close to $0{\cdot}47 \times 20$ cm/s, while the velocity of the head of the animal is $0{\cdot}088 \times 20$ cm/s. The value of V/U is therefore

$$\frac{V}{U} = \frac{0{\cdot}088}{-0{\cdot}47 + 0{\cdot}088} = -0{\cdot}23.$$

The value of B/λ is found to be approximately 0·18. The point $B/\lambda = 0{\cdot}18$, $V/U = -0{\cdot}23$ is shown in figure 10 as the point W. It will be seen that this point corresponds with a value $[C_D]_p/C_f$ rather less than 0·5, so that the longitudinal force coefficient is more than twice as great as the transverse coefficient. It is doubtful whether the type of roughness which this animal possesses would confer on it the property that C_f is more than twice $[C_D]_p$ if the roughness consisted of rigid projections. In fact the roughness consists of flexible projections which the animal moves in the same direction as that of the surface itself in places where that surface is moving fastest, i.e. at the outside of the bends in its body. This increases the longitudinal force coefficient. The details of the movement were explained by Gray (1939*b*). The way in which each projection swings from left to right while the crest of a wave passes under it can be seen in figure 11.

Downloaded from https://royalsocietypublishing.org/ on 21 November 2023

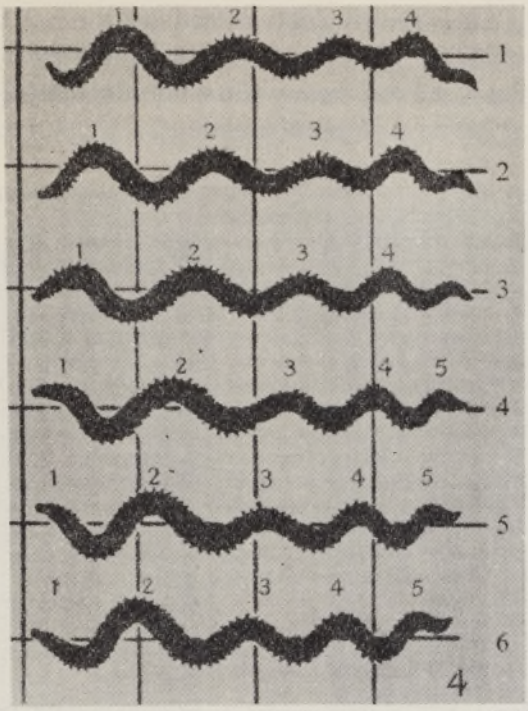

FIGURE 11. *Nereis diversicolor*, 20 frames per second (J. Gray).

9. LIMITATIONS TO THE APPLICATION OF THE ANALYSIS

In attempting to apply the analysis of the swimming of smooth animals it is necessary to bear in mind two kinds of limitation. In many animals the waves of displacement increase in amplitude as they pass from head to tail. It seems likely that such animals swim more efficiently than would be predicted by the analysis, but this question is not discussed here. The assumption that the force on each element of the flexible cylinder is the same as that on a similar portion of a long straight cylinder is likely to be inaccurate either when the diameter of the cylinder is comparable with the wave-length of the motion or when the Reynolds number associated with it is very low. Though it would be difficult to estimate theoretically the lower limit of Reynolds number above which the formulae might be expected to apply, the limiting-value of V/U when $R_1 = 0$ can be calculated. So far only the analysis for the case when B/λ is small has been given (Taylor 1952), and in that case

$$\frac{V}{U} = \tfrac{1}{2}B^2\left(\frac{2\pi}{\lambda}\right)^2 = \tfrac{1}{2}\tan^2\alpha. \tag{9·1}$$

In a private letter from Professor Lighthill I have learned that Mr G. J. Hancock, a worker in his department at Manchester University, has found that when B/λ is not small but d/λ is small, (9·1) must be replaced by an expression involving elliptic functions which has very nearly the same value as the algebraic expression

$$\frac{V}{U} = \frac{\tfrac{1}{2}\left(\frac{2\pi B}{\lambda}\right)^2}{1+\left(\frac{2\pi B}{\lambda}\right)^2} = \tfrac{1}{2}\sin^2\alpha. \tag{9·2}$$

Downloaded from https://royalsocietypublishing.org/ on 21 November 2023

The line representing (9·2) is shown chain-dotted in figure 4. It will be seen that this line lies close to the contour $[C_D]_p R_1^{\frac{1}{2}} = 10$, or approximately $R_1 = 100$ over its whole length. The part of figure 4 lying below the chain-dotted line has been shaded to show that points in it have no physical meaning.

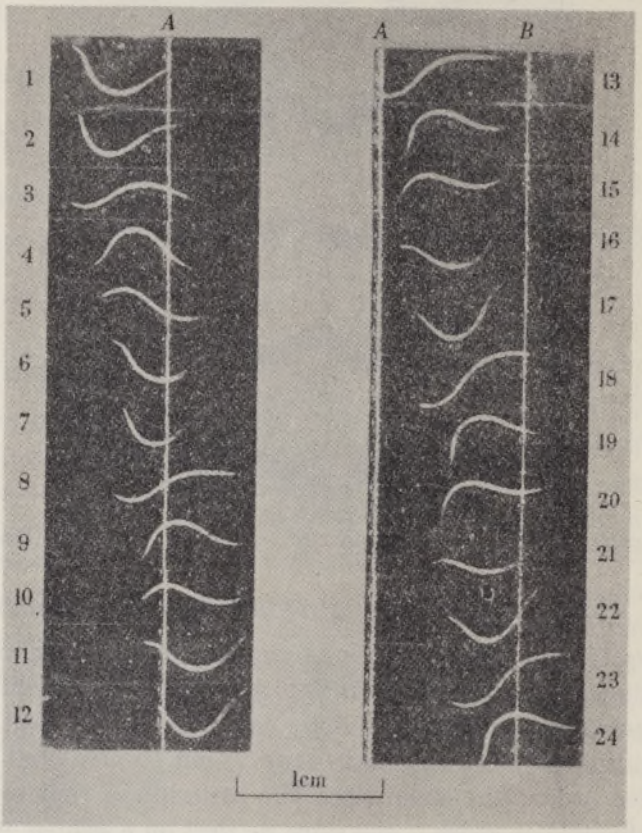

FIGURE 12. Ceratopogonid larva swimming, 40 frames per second (J. Gray).

On consulting Professor Gray as to the possibility that animals may be found whose swimming characteristics would be represented by a point in the swimming diagram near the chain-dotted limiting line, he showed me photographs, here reproduced as figure 12, which he had taken of a ceratopogonid larva. This animal is about 1 cm long. The time interval between successive frames in figure 12 is $\frac{1}{40}$ s. On measuring the photographs the following mean values were found:

$$V = 2{\cdot}17\,\text{cm/s}, \quad U = 7{\cdot}37\,\text{cm/s}, \quad \lambda = 0{\cdot}92\,\text{cm}, \quad d = 0{\cdot}038\,\text{cm}, \quad B = 0{\cdot}09\,\text{cm},$$

so that

$$R_1 = \frac{(7{\cdot}37)\,(0{\cdot}038)}{0{\cdot}011} = 25{\cdot}5.$$

If $[C_D]_p$ is taken as 1·0, $[C_D]_p R_1^{\frac{1}{2}} = 5$. The contour $[C_D]_p R_1^{\frac{1}{2}} = 5$ lies within the shaded portion of figure 4. The point representing the observations, namely, $\left(\frac{B}{\lambda} = \frac{0{\cdot}09}{0{\cdot}92} = 0{\cdot}1, \frac{V}{U} = \frac{2{\cdot}17}{7{\cdot}37} = 0{\cdot}3\right)$, is shown as C in figure 4. As would be expected it lies above the shaded portion.

Downloaded from https://royalsocietypublishing.org/ on 21 November 2023

My thanks are due to Professor James Gray for permitting the publication of figures 5, 7 and 12, which have not previously been published, and of figure 11, which is taken from a paper to which reference is made in the text. I am also grateful to him for suggestions made in the course of the work.

References

Blasius, H. 1908 *Z. f. Math. Phys.* **56**, 285.
Boussinesq, J. 1905 *J. Math. Pures appl.* 285.
Goldstein, S. 1938 *Modern developments in fluid dynamics*, p. 425. Oxford: Clarendon Press.
Gray, J. 1939*a* *Proc. Roy. Soc.* B, **128**, 28.
Gray, J. 1939*b* *J. Exp. Biol.* **16**, 9.
Gray, J. 1946 *J. Exp. Biol.* **23**, 101.
Gray, J. 1949 *J. Exp. Biol.* **26**, 354.
King, L. V. 1914 *Phil. Trans.* A, **214**, 373.
McLeod, A. R. 1918 *Rep. Memor. Aero. Res. Comm., Lond.*, no. 554.
Relf, E. F. & Powell, C. H. 1917 *Rep. Memor. Aero. Res. Comm., Lond.*, no. 307.
Sears, W. B. 1948 *J. Aero. Sci.* **15**, 49.
Taylor, Sir Geoffrey 1952 *Proc. Roy. Soc.* A, **211**, 225.
Thom, A. 1928 *Rep. Memor. Aero. Res. Comm., Lond.*, nos. 1176 and 1194.
Tomotika, S. & Aoi, T. 1951 *Quart. J. Mech. Appl. Math.* **4**, 401.
Wild, J. M. 1949 *J. Aero. Sci.* **16**, 41.

The effect of the temperature of preparation on the mechanical properties and structure of gelatin films

By E. Bradbury and C. Martin
The British Cotton Industry Research Association, Shirley Institute, Didsbury, Manchester

(*Communicated by Sir Eric Rideal, F.R.S.—Received* 24 *October* 1951—*Read* 28 *February* 1952—*Revised* 16 *April* 1952)

[Plate 4]

Gelatin films prepared by evaporation from aqueous solution at temperatures of 60° C and above differ considerably in structure and mechanical properties from films dried slowly at 20° C, when gelling precedes dehydration. In the high-temperature preparation dehydration precedes the formation of a continuous structure, and X-ray and other evidence indicates that the molecular chains are in a disordered contracted state not far removed from their condition in the sol. The high-temperature film is characterized by low strength and high recoverable extension under conditions of high relative humidity. In the low-temperature preparation the greater degree of crystallization has partially extended the molecular chains, and the unidirectional contraction of the film on drying has oriented them in the plane of the film. This film exhibits thermal contraction in hot methanol, and is stronger, but at high humidity is much less extensible, than the high-temperature preparation.

Of the adhesives used for sizing rayon textile yarns, gelatin is the most common, and probably more is known about its sizing and weaving behaviour than about that of other adhesives. It is thus a reasonable starting-point in a long-range

Downloaded from https://royalsocietypublishing.org/ on 21 November 2023